

## Novel Bayesian Additive Regression Tree Methodology for Flood Susceptibility Modeling

Janizadeh, Saeid; Vafakhah, Mehdi; Kapelan, Zoran; Dinan, Naghmeh Mobarghaee

**DOI**

[10.1007/s11269-021-02972-7](https://doi.org/10.1007/s11269-021-02972-7)

**Publication date**

2021

**Document Version**

Accepted author manuscript

**Published in**

Water Resources Management

**Citation (APA)**

Janizadeh, S., Vafakhah, M., Kapelan, Z., & Dinan, N. M. (2021). Novel Bayesian Additive Regression Tree Methodology for Flood Susceptibility Modeling. *Water Resources Management*, 35(13), 4621-4646. <https://doi.org/10.1007/s11269-021-02972-7>

**Important note**

To cite this publication, please use the final published version (if applicable). Please check the document version above.

**Copyright**

Other than for strictly personal use, it is not permitted to download, forward or distribute the text or part of it, without the consent of the author(s) and/or copyright holder(s), unless the work is under an open content license such as Creative Commons.

**Takedown policy**

Please contact us and provide details if you believe this document breaches copyrights. We will remove access to the work immediately and investigate your claim.

1 **Novel Bayesian Additive Regression Tree methodology for flood susceptibility**  
2 **modeling**

3 Saeid Janizadeh<sup>1</sup>, Mehdi Vafakhah<sup>1\*</sup>, Zoran Kapelan<sup>2</sup> and Naghmeh Mobarghaee Dinan<sup>3</sup>

4 <sup>1-</sup> Department of Watershed Management Engineering and Sciences, Faculty in Natural Resources and Marine  
5 Science, Tarbiat Modares University, Tehran, 14115-111 Iran, [janizadehsaeid@modares.ac.ir](mailto:janizadehsaeid@modares.ac.ir)

6 <sup>1-</sup> Department of Watershed Management Engineering and Sciences, Faculty in Natural Resources and Marine  
7 Science, Tarbiat Modares University, Tehran, 14115-111 Iran,\* Correspond author: [vafakha@modares.ac.ir](mailto:vafakha@modares.ac.ir)

8 2-Department of Water Management, Delft University of Technology, Delft, The Netherlands, [z.kapelan@tudelft.nl](mailto:z.kapelan@tudelft.nl).

9 3- Department of Environmental Planning and Design, Environmental Sciences Research Institute, Shahid Beheshti  
10 University, 1983969411 Tehran, Iran. [n\\_mobarghaee@sbu.ac.ir](mailto:n_mobarghaee@sbu.ac.ir)

11 **Abstract**

12 Identifying areas prone to flooding is a key step in flood risk management. The purpose of this  
13 study is to develop and present a novel flood susceptibility model based on Bayesian Additive  
14 Regression Tree (BART) methodology. The predictive performance of the new model is assessed  
15 via comparison with the Naïve Bayes (NB) and Random Forest (RF) based methods that were  
16 previously published in the literature. All models were tested on a real case study based in the Kan  
17 watershed in Iran. The following fifteen climatic and geo-environmental variables were used as  
18 inputs into all flood susceptibility models: altitude, aspect, slope, plan curvature, profile curvature,  
19 drainage density, distance from river distance from road, stream power index (SPI), topographic  
20 wetness index (TPI), topographic position index (TPI), curve number (CN), land use, lithology  
21 and rainfall. Based on the existing flood field survey and other information available for the  
22 analyzed area, a total of 118 flood locations were identified as potentially prone to flooding. The

23 data available were divided into two groups with 70% used for training and 30% for validation of  
24 all models. The receiver operating characteristic (ROC) curve parameters were used to evaluate  
25 the predictive accuracy of the new and existing models. Based on the area under curve (AUC) the  
26 new BART (86%) model outperformed the NB (80%) and RF (85%) models. Regarding the  
27 importance of input variables, the results obtained showed that the location's altitude and distance  
28 from the river are the most important variables for assessing flooding susceptibility.

29

30 **Keywords:** Flood susceptibility mapping; Bayesian; Regression Tree; Ensemble model; Bayesian  
31 Additive Regression Tree (BART);

## 32 **1. Introduction**

33 Any unforeseen natural occurrence that weakens or destroys economic, social and physical  
34 capacity, such as loss of life and finances, destruction of infrastructure, economic resources and  
35 areas of employment is defined as a natural disaster. Examples include earthquakes, floods,  
36 drought, seawater, volcanoes, landslides, hurricanes and natural pests (Vetrivel et al. 2018).  
37 Flooding is one of the most dynamic and disruptive natural events that puts human life and property  
38 and social and economic conditions at greater risk than any other natural disaster (Rahmati et al.  
39 2016; Yariyan et al. 2020). This phenomenon causes damage to human achievements at all times  
40 (Woodward et al. 2014; Darabi et al. 2019; Vafakhah et al. 2020). The highest risk of flooding and  
41 corresponding damage is in the populated, i.e. urban areas. In recent years, the increase in urban  
42 flood hazards, particularly along the river banks, has resulted in the risk of flooding for residents  
43 and movable property (Choubin et al. 2019). Due to the varying climate, unpredictable  
44 temperatures and rainfall in many of Iran's watersheds, several floods occur every year (Tehrany  
45 et al. 2014). Limiting environmental resources, reducing and destroying them as a result of the

46 expansion of human activities, poses many challenges for today's society and the next generation.  
47 The Kan watershed is affected by flooding events annually and this vulnerability has been  
48 documented (Hooshyaripor et al. 2020). Seven important flood events were recorded in this  
49 watershed since ..., causing damage to industrial, residential, agricultural land use, and fatalities,  
50 according to the available information.

51 Reducing human casualties as well as damage to property and the environment is a key objective  
52 shared by countries most often impacted by natural disasters. They are increasingly conducting  
53 feasibility studies with economic analysis to mitigate the effects of these disasters (Molinos-  
54 Senante et al. 2011). Although flooding cannot be prevented, the damage can be mitigated through  
55 appropriate analysis and forecasting techniques (Heidari 2014). The first step is to identify flood-  
56 prone areas (Janizadeh et al. 2019; Hosseini et al. 2020). One way to prevent and reduce flood  
57 damage is to provide people with reliable information through flood hazard zoning maps (Cook  
58 and Merwade 2009). The modelling of flood hazards, which may involve multi-temporal data sets,  
59 is required. Recently, machine learning methods have been successfully applied to assess flood  
60 risk with higher accuracy (Ngo et al. 2018; Talukdar et al. 2020). However, there is still no  
61 agreement on which method or set of methods can provide the best predictions (Kalantar et al.  
62 2021; Costache et al. 2021).

63 Rapid access to satellite imagery based on remote sensing data has increased the use of geographic  
64 information systems in the preparation of flood susceptibility maps. A wide range of modelling  
65 techniques has been proposed and used in natural disaster assessment including AI based  
66 techniques (Sayers et al 2014). In recent years, Bayesian methods, partly because of their over-  
67 resistance to the presence of small sample sizes and ability to deal with missing or incomplete data,  
68 have been developed recently to model flood sensitivity. These include Naïve Bayes models (Liu

69 et al. 2016; Pham et al. 2020b; Tang et al. 2020) and regression tree models such as Random Forest  
70 (RF) models (Arabameri et al. 2020; Chen et al. 2020; Vafakhah et al. 2020), Decision Tree models  
71 (Khosravi et al. 2018; Costache 2019; Janizadeh et al. 2019; Pham et al. 2020a), Logistic  
72 Regression models (Shafapour Tehrany et al. 2017; Al-Juaidi et al. 2018; Tehrany and Kumar  
73 2018). These regression tree models have become popular in the research environment due to their  
74 capability to model nonlinear phenomena such as floods.

75 Machine learning algorithms by default usually present point estimates only, and so decisions are  
76 made ignoring the uncertainty surrounding these estimates. In recent years, the use of ensemble  
77 models has attracted the attention of researchers in various fields as ensemble models benefit from  
78 several individual models and therefore tend to have better performance than individual models  
79 (Al-Abadi 2018; Tehrany et al. 2019a; Costache and Bui 2020; Shahabi et al. 2020). Bayesian  
80 Additive Regression Tree is one of the new ensemble models that combines Bayesian and  
81 Regression tree algorithms giving the access to the full posterior distribution of all unknown  
82 parameters in the model. This can be useful to reduce the uncertainty.

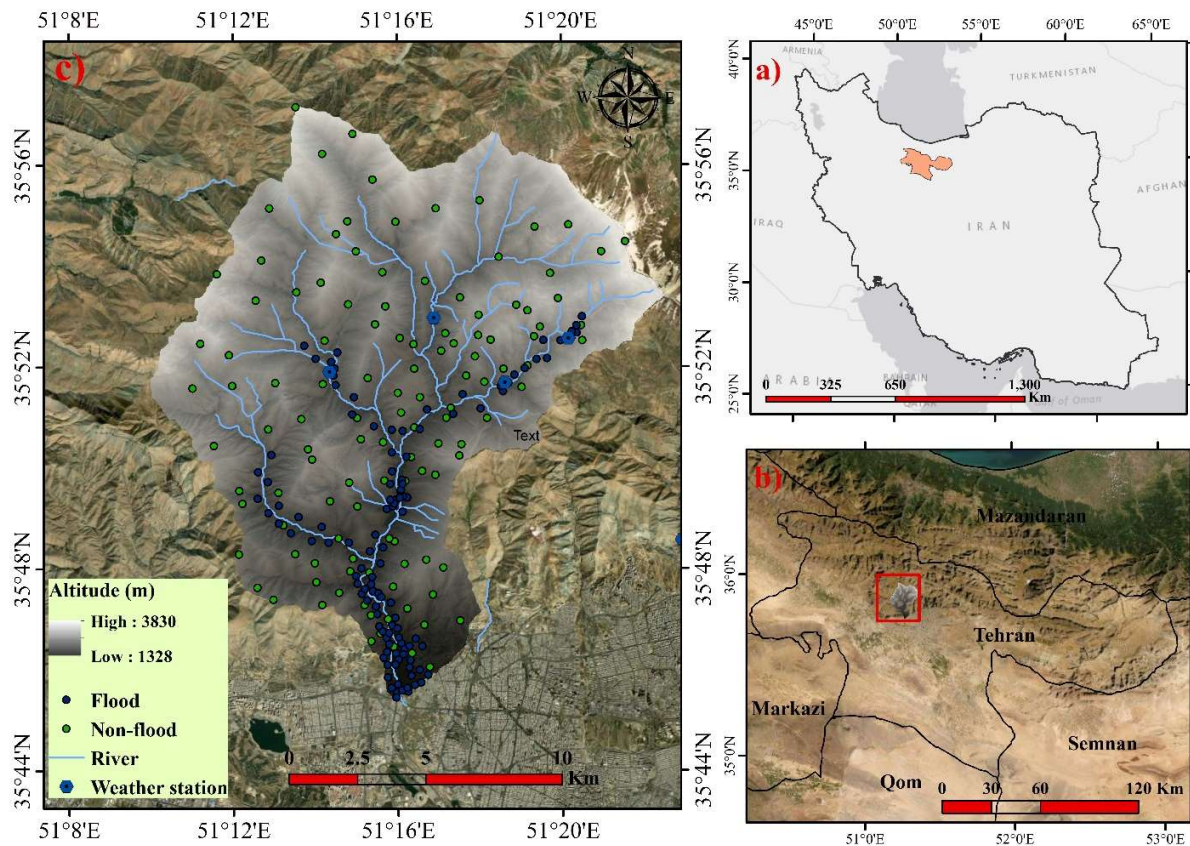
83 BART model has been used for modeling and predicting in different areas such as ecological  
84 processes (Plant et al. 2021) and gully erosion (Chowdhuri et al. 2020). Due to the fact that the  
85 flood is a non-linear phenomenon and has a lot of the uncertainty, use of appropriate models that  
86 have the ability to predict this phenomenon and reduce uncertainty is essential in the management,  
87 planning and prevention of flood risk. In the field of flood hazard modeling so far, very little  
88 attention has been paid to the role of hybrid Bayesian and Decision Tree algorithms. Therefore,  
89 the purpose of this study is to develop and present a new flood susceptibility model based on the  
90 ensemble type Bayesian Additive Regression Tree (BART) method. The new method will be

91 compared with the Naïve Bayes (Bayesian type) and Random Forest (regression tree type) based  
92 models to evaluate the predictive performance of the new method.

93

## 94 **1.2. Study area**

95 The Kan River watershed is 200 km<sup>2</sup> and is located northwest of Tehran, Iran. This watershed is  
96 located between latitudes 51° 10' and 51° 23' east and 35° 46' and 35° 58' north (Fig. 1). The  
97 average height of the watershed is 2428 meters, the average slope of the whole watershed is 43.4%  
98 and the most important river in this mountainous region is the Kan river. The study area is located  
99 in the southern margin of the central Alborz region in terms of geological status and has a  
100 mountainous climate with the average annual rainfall of 414.13 mm. The average annual discharge  
101 of the Kan River is 2.2 m<sup>3</sup>/s and its annual water flow is about 70 million m<sup>3</sup>/year. Seven important  
102 flood events have been reported in the Kan watershed since ..., which have caused damage to  
103 commercial and residential facilities, agricultural land and even caused casualties in the region  
104 (Delkash et al. 2014).



105

106

**Fig. 1. Location of case study a) country of Iran b) Tehran Province and c) Kan watershed**

107 **2. Material and methods**

108 **2.1. Flood Inventory Data Preparation**

109 In order to prepare a flood susceptibility map it is necessary to analyze the historical floods. The  
 110 Kan watershed has been severely affected by dangerous floods in recent decades, causing  
 111 extensive damage and casualties. According to historical floods recorded by the Regional Water  
 112 Company of Tehran Providence (1954/8/27, 1955/6/9, 1978/3/7, 1981/7/25, 1986/2/2, 1995/4/23,  
 113 1996/4/3), field visits and interviews with locals on 2019/10/5 to 2019/10/9 and the identification  
 114 of flood-affected areas by GPS equipment (Fig. 2), 118 flooding locations are identified in the  
 115 area. In addition to this, further 118 non-flood points were randomly placed in the inter-fluvial

116 area, or within very steep altitude where the flood phenomenon is almost impossible in the case  
117 study area. The position of all 236 locations are presented in Fig. 1. The data were divided into  
118 two categories of training and validation for modeling, so that 70% of the data were used for  
119 training and 30% for validation (Ahmadlou et al. 2019; Choubin et al. 2019). The flowchart of  
120 research methodology is given in Fig. 3.

121



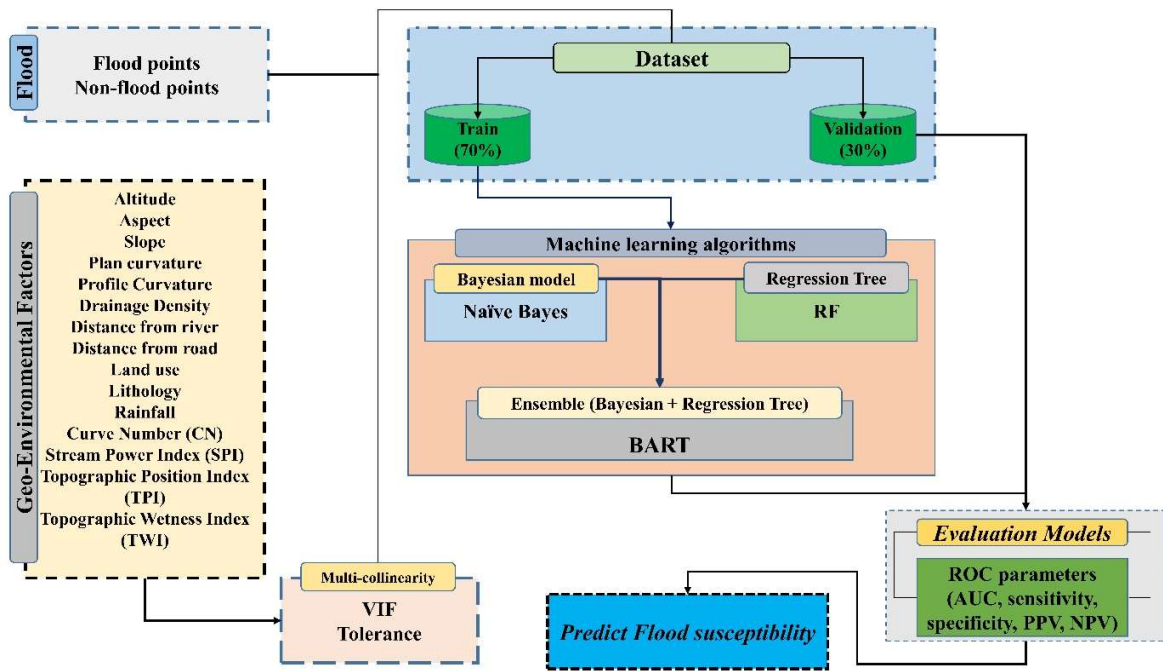
122

123

**Fig. 2. Example of a flood location in the Kan watershed**

124





125

126

Fig. 3. Research Methodology

127

## 128 2.2. Spatial Data Preparation

129 Floods are one of the natural phenomena and are affected by various climatic and geo-  
 130 environmental factors. In this study, the following 15 climatic and geo-environmental variables  
 131 are used as potential explanatory factors for flood susceptibility at a given location: altitude, aspect,  
 132 slope, plan curvature, profile curvature, drainage density, distance form river distance from road,  
 133 stream power index (SPI), topographic wetness index (TWI), topographic position index (TPI),  
 134 curve number (CN), land use, lithology and annual rainfall (Ngo et al. 2018; El-Magd et al. 2021).

135 The above 15 factors (i.e. potential flood susceptibility model independent variables) were  
 136 confirmed as significant by using the multi-collinearity analysis. The multi-collinearity analysis  
 137 evaluates the intensity of multiple correlations between considered variables by calculating the

138 variance inflation factors (VIFs). The higher the value of the VIF the more likely it is that that  
139 variable does not play a significant role in flood susceptibility prediction (Miles 2014). In this  
140 study, the threshold of 5 was used for VIF to identify significant independent variables (Tehrany  
141 et al. 2019a; Hosseini et al. 2020). VIFs were estimated using the USDMM package in R software.  
142 The analysis has shown that all fifteen variables shown here have VIF values below the above  
143 threshold (see section 4.1) hence they have all been used a potential explanatory factors for  
144 predicting the flooding susceptibility.

145 The values of above 15 variables were prepared based on previous studies (see Fig 4, 5 and 6). For  
146 this purpose, the digital elevation model (DEM) of the study area with resolution of 12.5×12.5 m  
147 was developed with elevation data obtained using the type L-band Synthetic Aperture Radar  
148 (PALSAR) (<https://vertex.daac.asf.alaska.edu/#>). The aspect map was prepared based on DEM at  
149 nine class in the ArcGIS 10.5 software (Choubin et al. 2019; Janizadeh et al. 2019). The ground  
150 slope is one of the important factors in the occurrence of floods in watersheds (Tehrany et al. 2015;  
151 Chapi et al. 2017). The slope map was prepared based on the DEM in ArcGIS 10.5 software  
152 (Khosravi et al. 2018).

153 The plan and profile curvature are the spatial parameters used in the preparation of flood maps of  
154 watersheds. These variables were prepared in ArcGIS 10.5 software using a DEM (Rahmati et al.  
155 2016; Hong et al. 2018). Drainage density of the study area in ArcGIS 10.5 environment was based  
156 on line density extension (Mahmoud and Gan 2018; Zhao et al. 2019). Distance from rivers is one  
157 of the most important factors affecting flooding of lands along the rivers (Tehrany et al. 2014;  
158 Khosravi et al. 2016, 2018). This map was prepared using the Euclidean order in ArcGIS 10.5  
159 software (Khosravi et al. 2018). Distance from the road is also a factor affecting flooding. This

160 variable was prepared using the 1:50,000 road map of Tehran province, the ArcGIS10.5 software  
161 and the Euclidean extension, to determine distance from the road (Shafapour Tehrany et al. 2017).

162 The stream power index (SPI) is one of the important parameters for flooding in watersheds and  
163 the following relationship is defined here (Tehrany et al. 2014; Shafizadeh-Moghadam et al. 2018):

$$164 \quad SPI = Catchment Area * \tan(slope) \quad (1)$$

165 System for Automated Geoscientific Analyses Geographic Information System (SAGA GIS 2.6)  
166 software was used to prepare this variable (Tehrany et al. 2014).

167 Topographic position index (TPI) indicates the topographic status of the area, with positive values  
168 indicating high altitudes and negative values indicating low altitudes such as valleys (Papaioannou  
169 et al. 2015). Due to the role of topographic shape in the formation of floods, this index is considered  
170 as one of factors affecting floods and this variable was prepared using the SAGAGIS 2.6 software.  
171 TWI measures the effect of local topography on runoff production and shows the long-term  
172 moisture content of a landscape (Hong et al. 2018; Khosravi et al. 2019), hence this indicator is  
173 one of the influential variables in flood risk assessment in watersheds. This variable was obtained  
174 based on the following (Khosravi et al. 2019) in SAGAGIS 2.6 software:

$$175 \quad TWI = \ln(Catchment Area / \tan(slope)) \quad (2)$$

176 Lithology is one of the important factors in watershed flooding due to its direct effect on the level  
177 of permeability and surface runoff (Rahmati et al. 2016). The geological map of the Kan watershed  
178 was prepared based on the 1:100,000 geological map of the Iranian National Cartographic Center  
179 (NCC) and then turned into a raster layer with a resolution of 12.5 m. The lithology map of the  
180 study area was divided into seven different classes. The soil type map was also prepared using the  
181 data from the Administration of Natural Resources of Tehran Province and the vector file of this

182 map was created with a raster format with pixel size of 12.5 meters using the ArcGIS 10.5 software  
183 (Tehrany et al. 2014).

184 Land use is the result of the interrelationships of socio-cultural parameters and the potential of the  
185 land (Rahmati et al. 2016; Bui et al. 2018). Changes in land use and land cover can have significant  
186 impact on flooding in watersheds (Khosravi et al. 2018). This map was prepared using images of  
187 Landsat 8 satellite imagery OLI sensors in 2019 and using the maximum likelihood algorithm and  
188 supervised classification in the ENVI 5.1 software and divided into four classes: orchard,  
189 rangeland, residential and rocky lands.

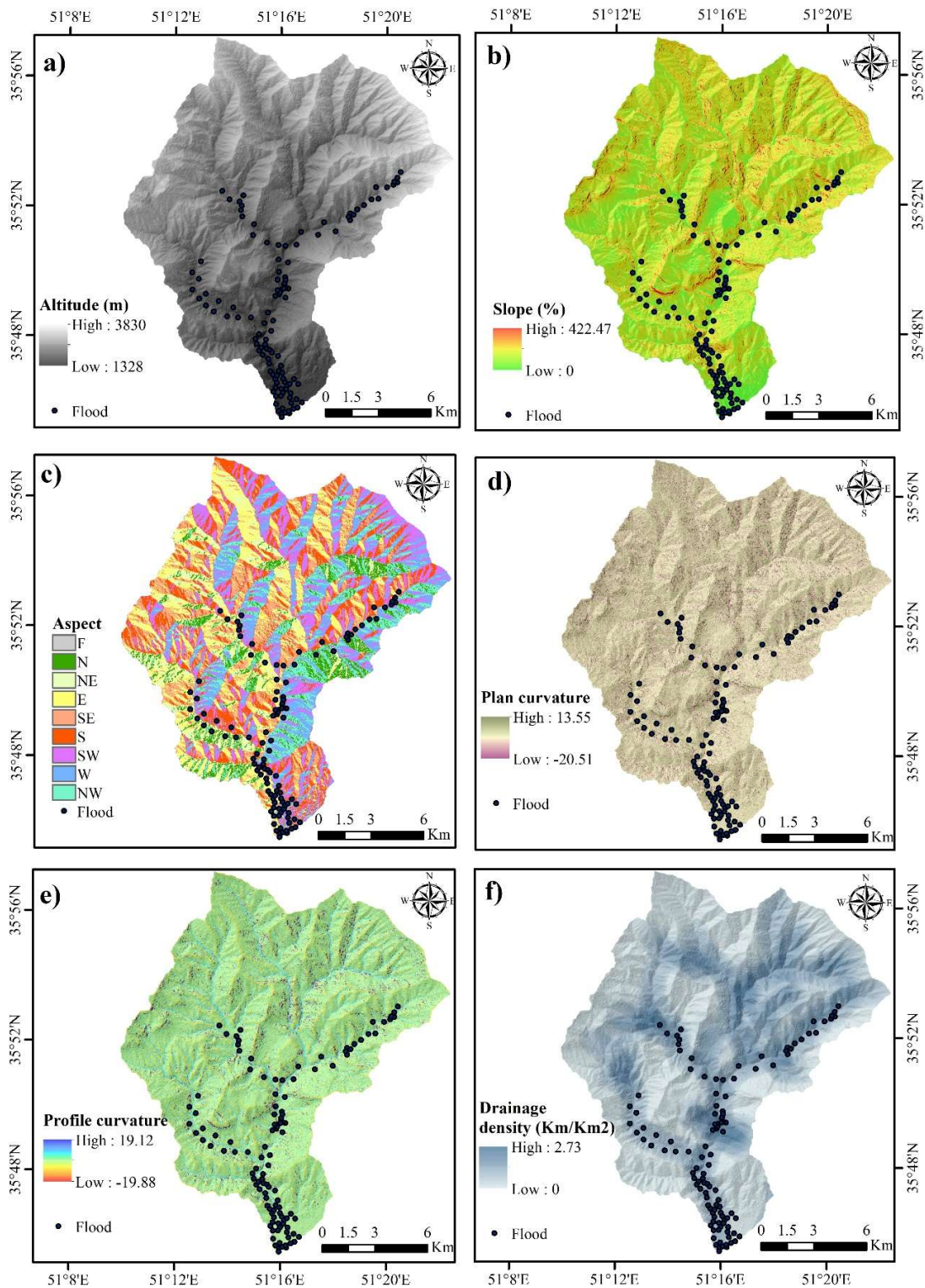
190 In order to prepare the annual rainfall map, the rainfall data of 7 gauge stations (inside and outside  
191 the watershed) were used in the period 1994-2019. After carefully examining the various  
192 interpolation methods in the ArcGIS 10.5 software, the distribution of annual rainfall in Kan  
193 watershed was prepared based on the ordinary Kriging method.

194 One of the most important factors in the occurrence of floods is soil condition and different land  
195 uses, which directly affects the amount of water infiltration into the land. In other words, the curve  
196 number (CN) at the level of each area indicates the hydrological behavior of that area and its  
197 discharge regime during rainfall. In order to determine the CN map the land use map and the  
198 hydrological soil groups map were combined in the ArcGIS software environment. Then, based  
199 on the tables related to the CN for different land uses of watersheds and according to hydrological  
200 soil groups map, the value of CN was determined in the case of previous average humidity  
201 (Mahmoud and Gan 2018; Tang et al. 2018).

202 The data summary information of all independent variables is shown in Table 1.

203 Table 1. Information of independent variables

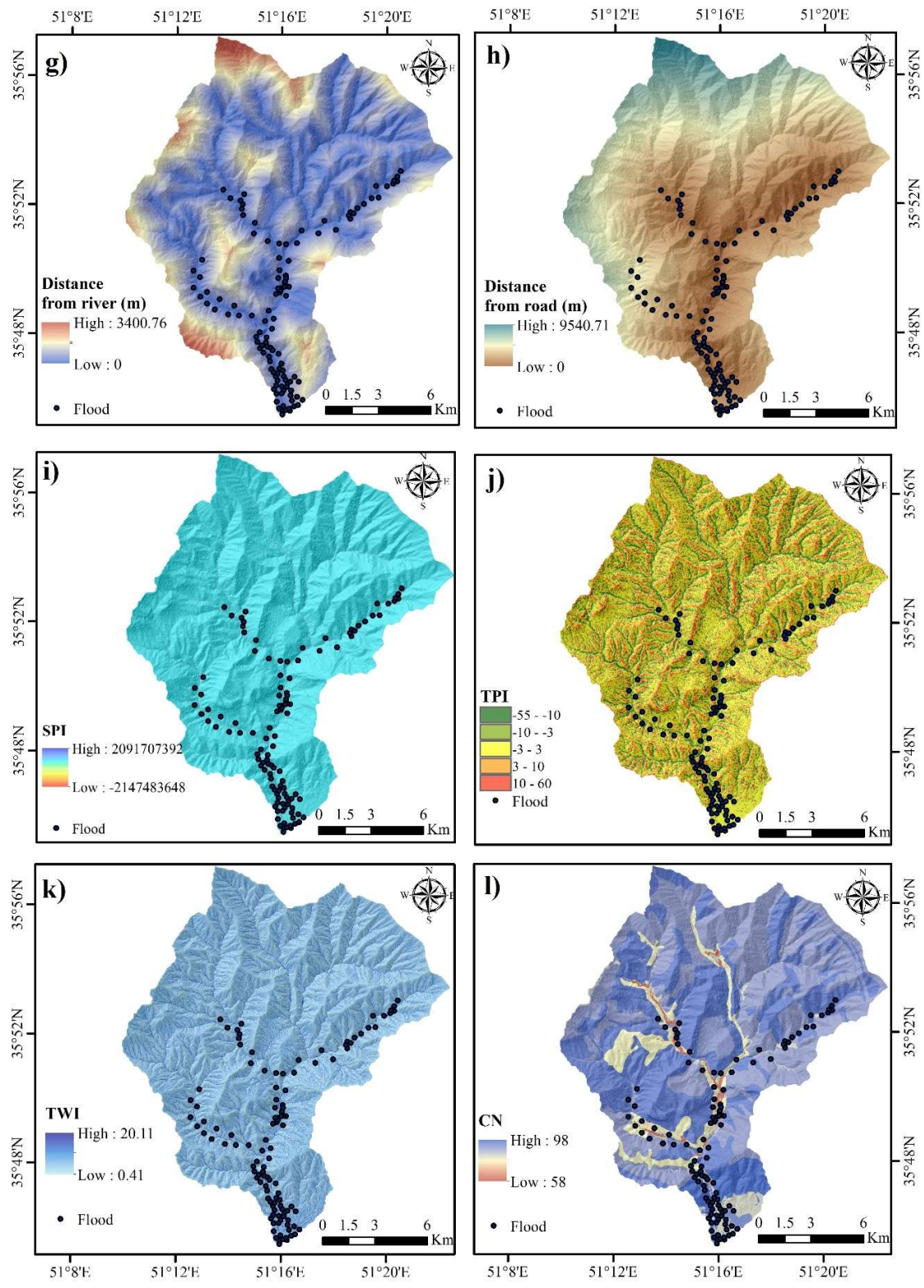
Variables	Data Type	Data Source	Data resolution
Elevation	Raster Grid	ALOS PALSAR DEM, (Alaska Satellite Facility)	12.5 m* 12.5 m resolution
Aspect			
Slope			
Plan Curvature			
Profile Curvature			
Drainage Density			
SPI			
TWI			
TPI			
Distance from River	Line and polygon coverage	Administration of Natural Resources, Department Tehran Province.	1:50000
Distance from Road	Line and polygon coverage		1:50000
LULC	Spatial/Raster grid	Landsat 8 OLI (USGS)	30 m spatial resolution
Lithology	Line, point and polygon coverage	Geological Map by country's mapping organization (Iran)	1: 100000
Rainfall	Station specific information	25 Years information of rain gage stations	Interpolation with same spatial resolution with other parameters
CN	Raster Grid	LULC and hydrological soil groups map	



205

206  
207

Fig 4. Flood conditioning factors: a) altitude, b) aspect, c) slope, d) plan curvature, e) profile curvature, f) drainage density

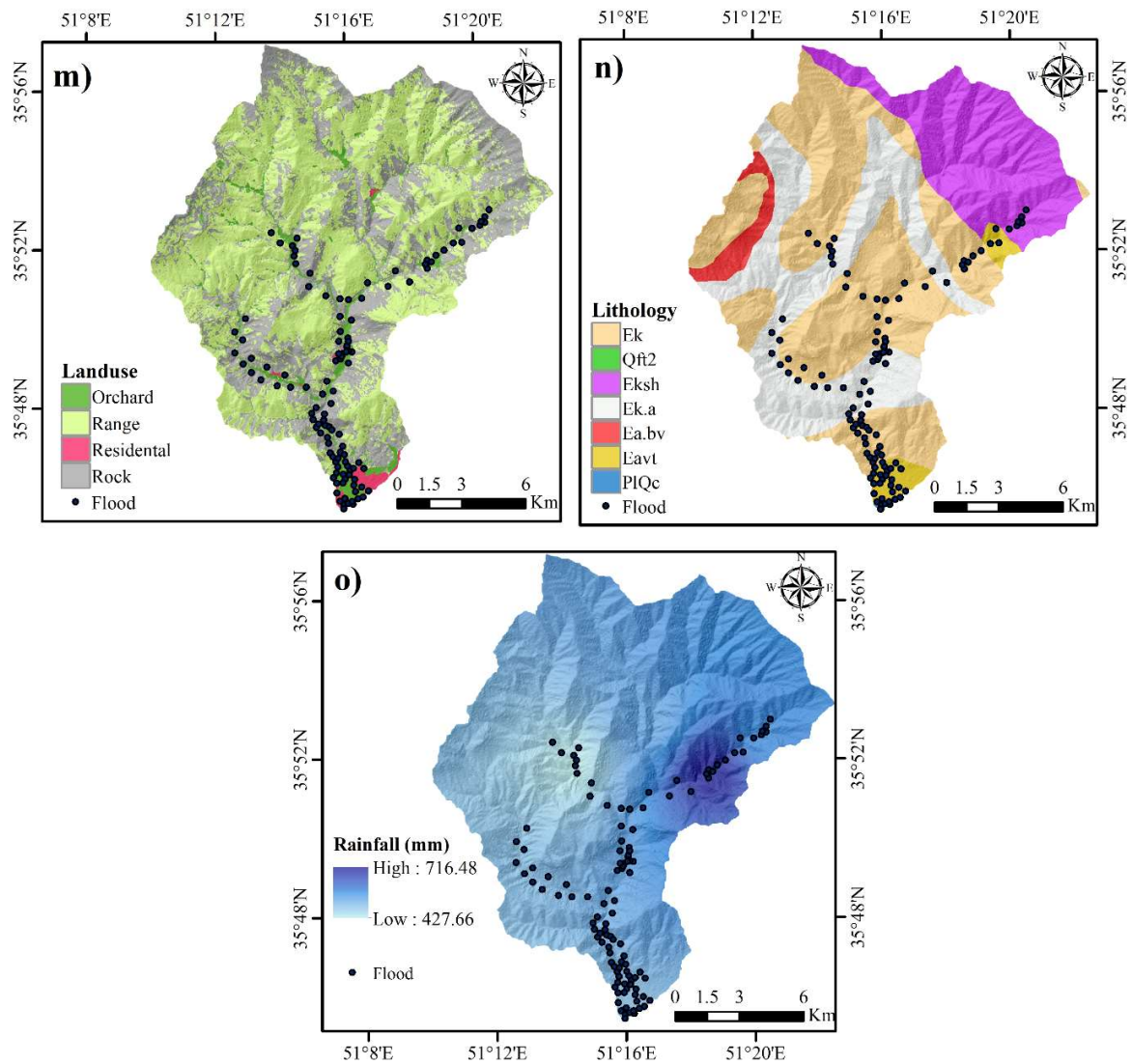


208

209 **Fig 5. Flood conditioning factors: g) distance from river, h) distance from road, i) SPI, j) TWI, k) TPI, l) CN**

210

211



212

213

Fig. 6. Flood conditioning factors: m) land use, n) lithology and o) annual rainfall

### 214 2.3. Flood susceptibility models

215 This section describes three different models for predicting flood susceptibility: BART, NB and  
216 RF. All models are based on different machine learning methods that predict the flood  
217 susceptibility defined as the probability of flood occurrence at a given location of the analyzed



218 watershed. All three models have the same set of input variables, the fifteen explanatory /  
219 independent variables described in section 2.3. These model inputs were determined in all cases  
220 using correlation and multi-collinearity analysis (see next section). Finally, all models are trained  
221 and tested using the data described in the next section.

222

### 223 **2.3.1. Naïve Bayes Model**

224 The Bayesian method is a way of classifying phenomenon based on the probability of that  
225 phenomenon occurring or not occurring. Based on the inherent characteristics of probability  
226 (especially probability division), Naive Bayes method offers good results after receiving the initial  
227 practice (Rish and others 2001). Learning method in the simplest way, the base is the type of  
228 learning with the supervisor. Bayes suggests a way to calculate the posterior probability,  $P(c|x)$ ,  
229 from  $P(c)$ ,  $P(x)$  and  $P(x|c)$ . The Naive Bayes classifier assumes that the effect of the predictor  
230 cost ( $x$ ) on a given category ( $c$ ) of the different predictor values is neutral. This assumption is  
231 known as conditional independence:

$$232 \quad P(c|x) = \frac{P(c|x)*P(c)}{P(x)} \quad (3)$$

$$233 \quad P(c|X) = P(x_1|c) * P(x_2|c) * \dots * P(x_n|c) \quad (4)$$

234 where  $P(c|x)$  is posterior probability of target,  $P(c)$  is prior probability of class and  $P(x)$  is the  
235 prior probability of predictor (Zhang 2004). The e1071 package in R software was used for Naïve  
236 Bayes modeling.

### 237 **2.3.2. Random Forest Model**

238 Random Forest (RF) method is a relatively complex method in which several decision trees are  
239 trained in order to increase the predictive accuracy of the model. The result is a prediction of a  
240 group of decision trees. In the random forest learning method, each decision tree is taught using a  
241 random sample selected from the training data set. The total selection of predictive variables used  
242 to divide nodes is also random. In the random forest method, the two properties *mtry* and *ntree* are  
243 determined for the number of auxiliary variables used in each subset and the number of trees used  
244 in the forest, respectively. One of the advantages of a random forest is that it can be used for both  
245 classification and regression type models. Random forest has parameters similar to the decision  
246 tree or "Bagging Classifier". Random forest adds randomness to the model as trees grow. Instead  
247 of searching for the most important features when dividing a "node", this algorithm looks for the  
248 best features among a random set of features. This leads to more variety and ultimately a better  
249 model. Therefore, in a random forest, only one subset of features is considered by the algorithm to  
250 divide a node. By adding a random threshold for each attribute, instead of searching for the best  
251 possible threshold, trees can be made even more random (Liaw et al. 2002). The randomForest  
252 package in R software was use for the RF modeling here.

### 253 **2.3.3. Bayesian Additive Regression Tree (BART) Model**

254 BART is a Bayesian approach to non-parametric output estimation using regression trees. The  
255 regression trees are relying on the return of the binary division of the predictive space into a set of  
256 superconductors to approximate certain unknown functions. The predictive space has dimensions  
257 corresponding to the number of variables. Tree-based regression models are capable of generating  
258 plenty of interaction and nonlinearity (Hill et al. 2020). Models consisting of a number of  
259 regression trees are more capable of capturing interaction and nonlinearity than single trees, as are  
260 additives in f.

261 BART can be considered a general collection of trees with a new estimation method based on a  
262 complete Bayesian probability model. The BART model can be expressed as follows:

$$263 \quad P(Y = 1|X) = \varphi(\tau_1^N(X) + \tau_2^N(X) + \dots + \tau_n^N(X)) \quad (5)$$

264 where  $\varphi$  denotes the cumulative density attribute of the prevalent regular distribution. In this  
265 formulation, the sum-of-trees model serves as an estimate of the conditional probit at  $x$  which can  
266 be besides issues modified into a conditional threat estimate of  $Y = 1$  (Kapelner and Bleich 2013).  
267 The `bartMachine` package in R software was use for BART modeling.

#### 268 **2.3.4. Model Validation and Performance Assessment**

269 The ROC curve characterizes the relative performance of each model. The ROC curve is a graph  
270 in which the true positive (or specificity value) is shown in the vertical axis whilst the false positive  
271 (or sensitivity) is shown on the vertical axis (Fratini et al. 2010). For the sensitivity or a proportion  
272 of occurrence pixels that have been correctly predicted, the larger this value the more accurate the  
273 model is in determining the occurrence points. Also, the feature means a ratio of non-occurring  
274 pixels that the model correctly predicted. The area under the curve (AUC) measures one aspect of  
275 performance. The value of AUC varies from 0 to 1, where the value of 0.5 denotes the random  
276 prediction and 1 denotes the perfect prediction (Yesilnacar and Topal 2005). In this study, the  
277 following equations have been used to calculate true positive rate (TPR), true negative rate (TNR),  
278 specificity, sensitivity and AUC:

$$279 \quad TPR = \frac{TP}{(TP+FN)} \quad (6)$$

$$280 \quad TNR = \frac{TN}{(TN+FP)} \quad (7)$$

281 
$$\text{Sensitivity} = \frac{\text{Number of positives}}{(\text{Number of positives} + \text{Number of false positives})} \quad (8)$$

282 
$$\text{Specificity} = \frac{\text{Number of true negatives}}{(\text{Number of true negatives} + \text{Number of false negatives})} \quad (9)$$

283 
$$\text{AUC} = \frac{\sum TP + \sum TN}{(P + N)} \quad (10)$$

284 where, TP (true positive) and TN (true negative) are truly classified pixel numbers, while FP (false  
 285 positive) and FN (false negative) are falsely classified pixel numbers; P is the total number of  
 286 floods and N is the total number of non-floods (Choubin et al. 2019; Khosravi et al. 2019).

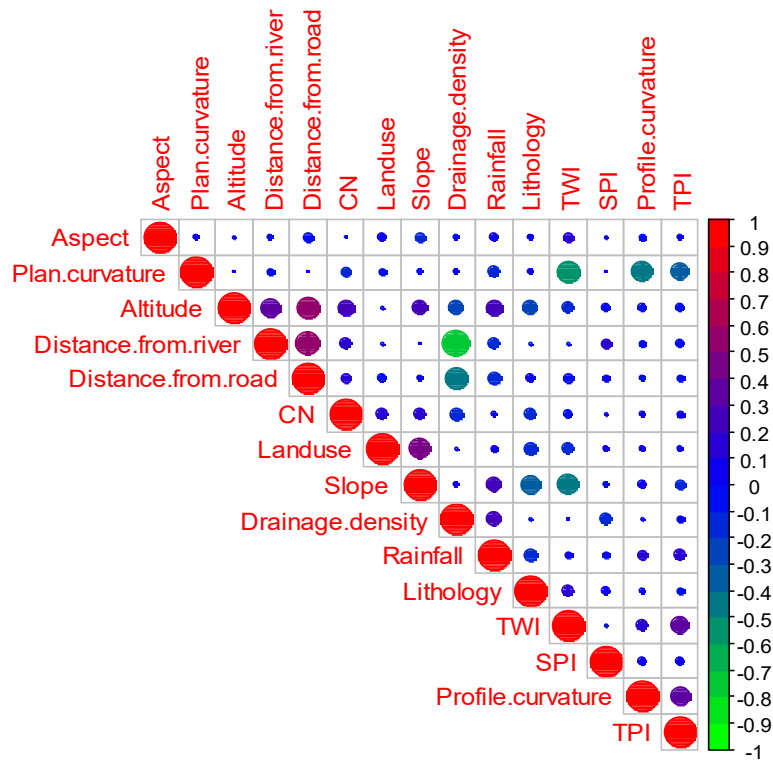
287

### 288 **3. Results**

#### 289 **3.1. Analysis of Independent Variables**

290 In order to build a flood susceptibility model, potential model input variables are first analyzed for  
 291 independence (via correlation) and linearity (via multi-collinearity analysis).

292 The results of the correlation study of the variables used in flood susceptibility modelling based  
 293 on Spearman correlation test are shown in Fig.7. As it can be seen from this figure, the analyzed  
 294 variables have a relatively low correlation with each other hence these were all selected for further  
 295 analysis.



296

297

**Fig. 7. Correlation analyses between independent variables**

298

299 In order to determine the appropriate inputs for flood susceptibility modelling, multiple  
 300 multiplexing and tolerance tests were used using *usdm* package (in the R software environment).

301 In order to investigate the linearity of the VIF range, all variables with VIF value smaller than 5  
 302 were considered.

303 The results of multi-colinearity and tolerance analyses are shown in Table 2. The study of the  
 304 linearity of the variables shows that all analyzed variables have a VIF value smaller than 5. The  
 305 highest linearity was obtained for distance from the river with VIF equal to 2.39 and the tolerance  
 306 equal to 0.42. The smallest linearity was obtained for the aspect variable with VIF of 1.07 and

307 tolerance of 0.93. Based on this, all variables shown in Table 2 are selected as potential inputs into  
 308 the flood susceptibility model.

309 **Table 2. Multi-collinearity analysis base on VIF and Tolerance to determine the linearity of the independent**  
 310 **variables**

<b>Variables</b>	<b>VIF</b>	<b>Tolerance</b>
Altitude	2.09	0.48
Aspect	1.07	0.93
Slope	1.57	0.64
Plan curvature	1.9	0.53
Profile Curvature	1.47	0.68
Drainage density	2.33	0.43
Distance from River	2.39	0.42
Distance from road	2.09	0.48
SPI	1.09	0.92
TPI	1.37	0.73
TWI	2.01	0.50
CN	1.35	0.74
Land use	1.29	0.77
Lithology	1.27	0.79
Rainfall	1.46	0.68

311

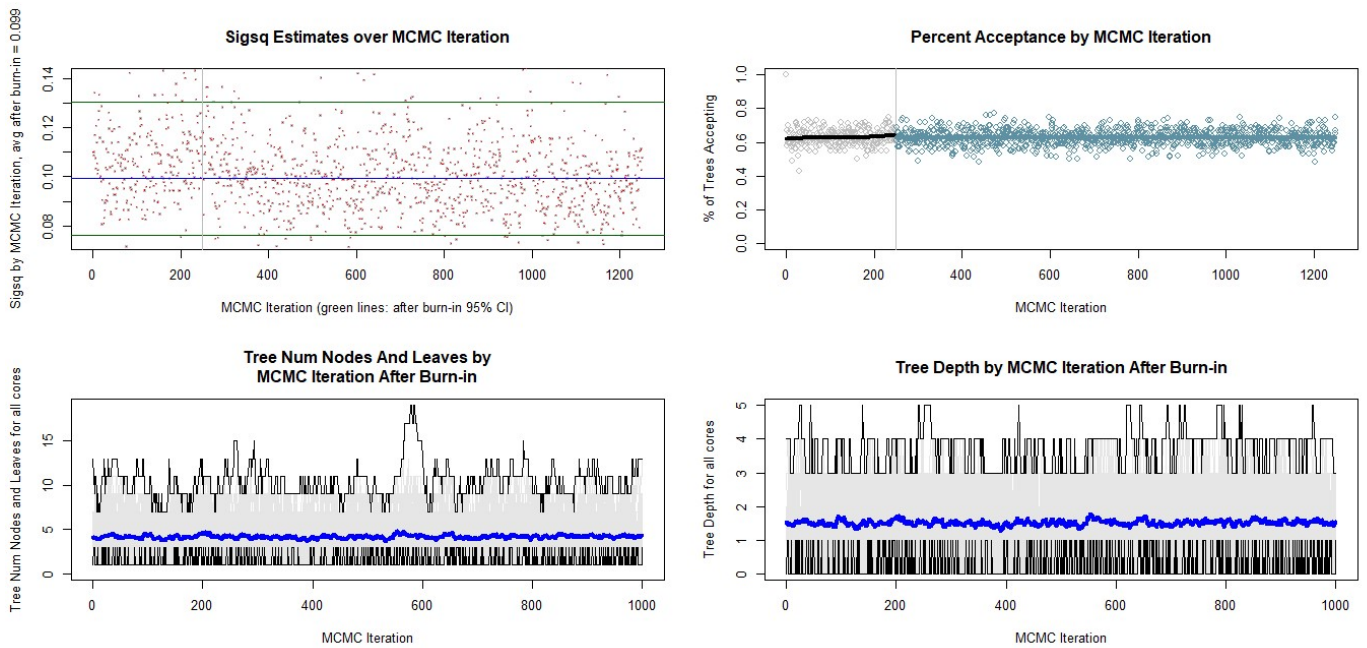
### 312 **3.2. Tuned parameters**

313 The tuned parameter values for the BART model are shown in Table 3 and Figure 8.

314 **Table 3. Tune parameters in BART model**

<b>Parameters</b>	<b>Tuned value</b>
Number of trees	100
Number burn in	500
Number iteration after burn in	1000
Alpha	0.95
Beta	2
K	2
Q	0.9

315



316

317

**Fig. 8. The result of the BART model for flood susceptibility**

### 318 **3.3 Model Validation**

319 ROC curves parameters include sensitivity, specificity, NPV, PPV and area under curve (AUC).

320 These parameters were used to evaluate the efficiency of Naïve Bayes, RF and BART models. The

321 corresponding results for the training and testing stages of these models are shown in Figs. 9 and

322 10 and Table 4.

323 According to the results obtained in the training phase, the sensitivity statistics in NB, RF and

324 BART models are equal to 0.76, 0.99 and 0.99, respectively. This shows the high sensitivity of the

325 three models and their accuracy. The specificity statistics for the NB, RF and BART models are

326 equal to 0.89, 0.95 and 0.90, respectively. The PPV statistics of 0.74, 0.95 and 0.91 and the NPV

327 statistics of 0.77, 0.99 and 0.98 were obtained for the NB, RF and BART models, respectively.

328 This shows the high accuracy of these models in predicting the non-occurrence points. The results

329 of model evaluation based on the AUC show that the accuracy of NB, RF and BART models is

330 0.88, 0.99 and 0.89, respectively. Therefore, all three models have high predictive accuracy at the  
 331 training stage.

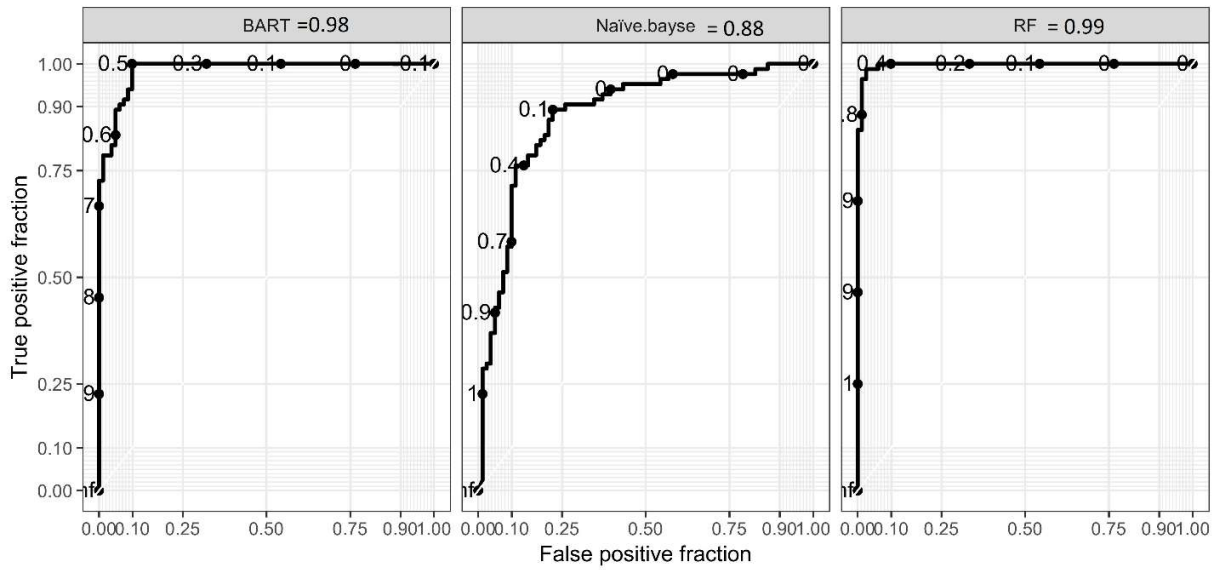
332 Evaluation of the three models at the validation stage shows that the sensitivity statistics for NB,  
 333 RF and BART models are equal to 0.76, 0.91 and 0.94, respectively. This shows the high  
 334 sensitivity of these models in flood estimation. The specificity statistics in the NB, RF and BART  
 335 models are equal to 0.75, 0.72 and 0.78, respectively. Evaluation of the same three models based  
 336 on PPV and NPV statistics result in PPV values of 0.74, 0.75, 0.80, and NPV values of 0.77, 0.90,  
 337 and 0.93 respectively, indicating high accuracy of these models when predicting non-flood points  
 338 compared to flood points. For the overall evaluation of the models at the validation stage, the AUC  
 339 statistic was used too and the values obtained for the NB, RF and BART models are equal to 0.81,  
 340 0.85 and 0.89, respectively.

341 **Table 4. The results of evaluating the efficiency of Naïve Bayes, RF and BART models in train and validation**  
 342 **stage**

Models	Stage	Parameters				
		Sensitivity	Specificity	PPV	NPV	AUC
Naïve	Train	0.76	0.89	0.87	0.78	0.88
Bayes	Validation	0.76	0.75	0.74	0.77	0.81
RF	Train	0.99	0.95	0.95	0.99	0.99
	Validation	0.91	0.72	0.75	0.90	0.85
BART	Train	0.99	0.90	0.91	0.98	0.98
	Validation	0.94	0.78	0.80	0.93	0.89

343



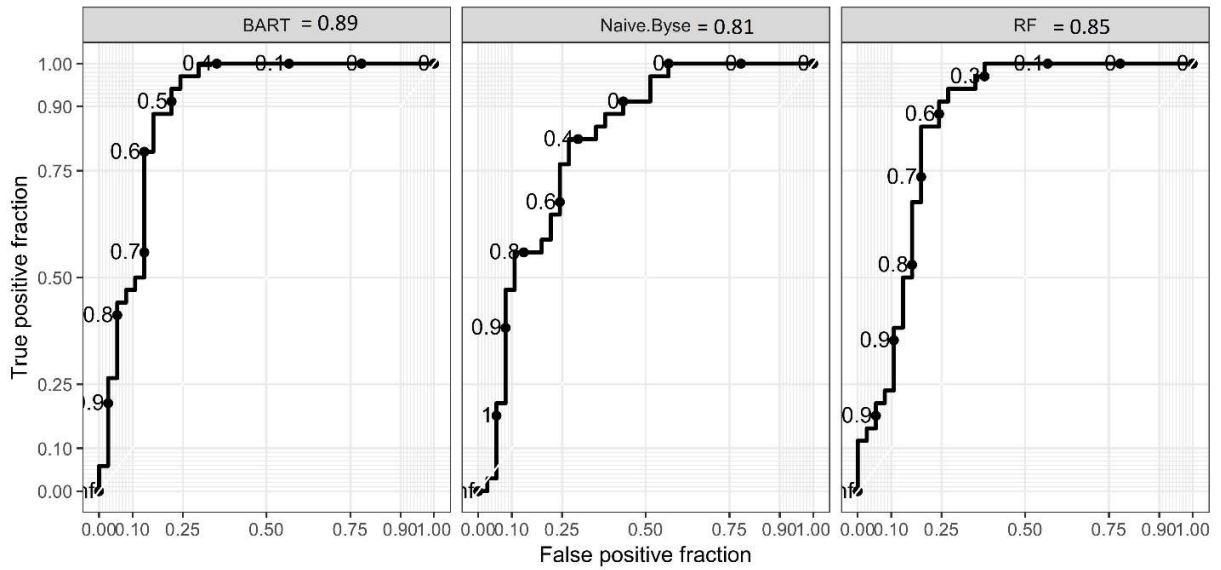


344

345

**Fig. 9. The ROC curve analysis for Naïve Bayes, RF and BART models using the train dataset**

346



347

348

**Fig. 10. The ROC curve analysis for Naïve Bayes, RF and BART models using the testing dataset.**

349

350

351

352

### 353 **3.4. Flood susceptibility modeling results**

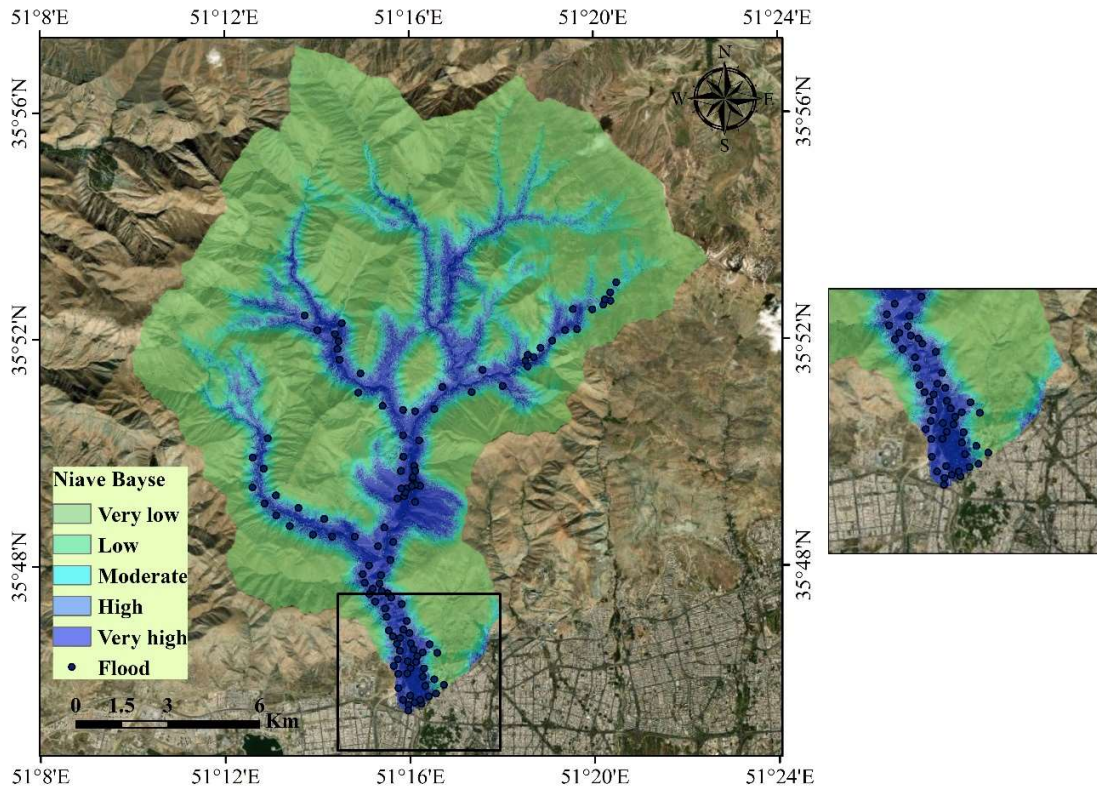
354 After modelling the flood sensitivity using NB, RF and BART models and evaluating the  
355 efficiency of these models, flood susceptibility was forecasted for the whole analyzed watershed.

356 The final map was divided into five flooding susceptibility classes (very low, low, moderate, high  
357 and very high) by using the natural break algorithm (Fig. 11). According to the map obtained,  
358 flooding susceptibility is the highest sensitivity around the main river and the areas near the outlet  
359 of the watershed, which have a lower altitude. At the same time, most of the area analyzed, which  
360 is generally high altitude, has a very low sensitivity.

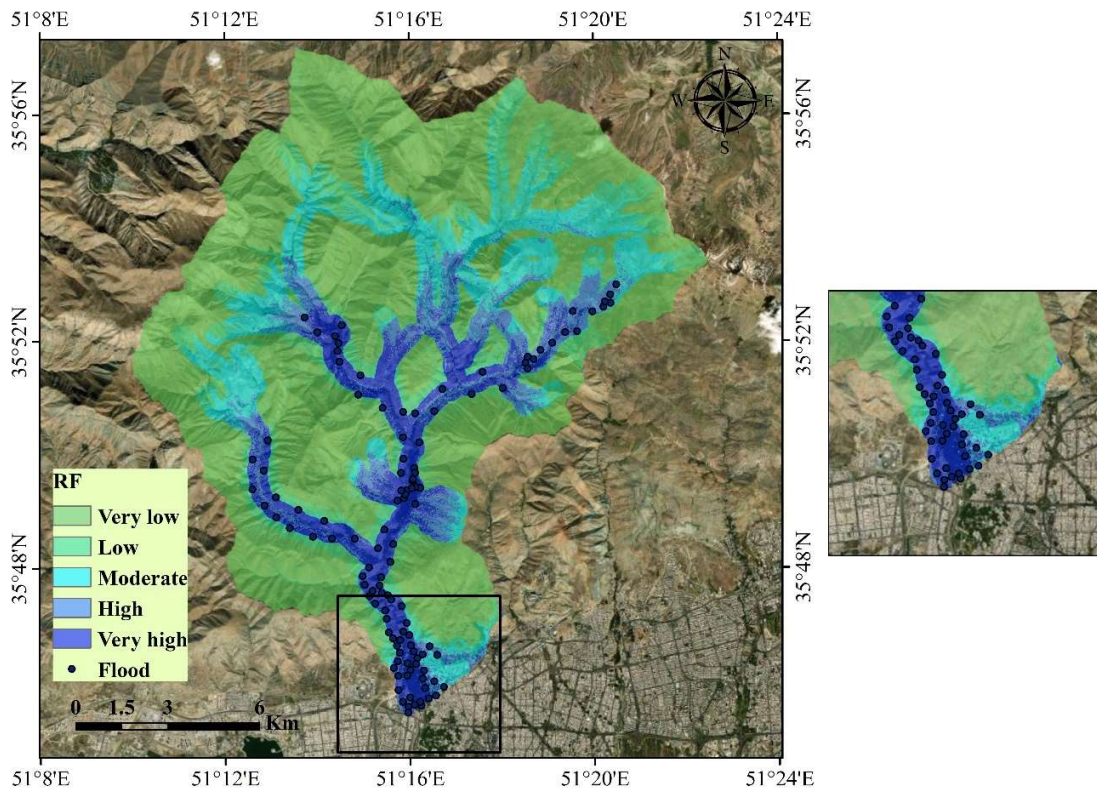
361 The results of the area and percentage covered by each susceptibility class are shown in Table 5.  
362 According to the results, the area of very high susceptibility class is equal to 22.11 km<sup>2</sup> (10.26%)  
363 in the NB model, 21.23 km<sup>2</sup> (9.85%) in the RF model and 19.48 km<sup>2</sup> (9.04%) in the BART model.  
364 However, the BART model, with 50.5 km<sup>2</sup> (23.5%) has predicted the largest area with very high  
365 and high susceptibility classes.

366 In order to evaluate the validity of the predicted flood susceptibility maps in relation to the  
367 identified flood points in the study area, the frequency ratio (FR) approach was used (Fig. 9). As  
368 it can be seen from Figure 12, the highest frequency ratio is in very high and high classes, which  
369 indicates the appropriate prediction of the models used for flood-susceptibility areas. However,  
370 the predictions of the RF and BART models that are in the very high class are much higher than  
371 the corresponding class predictions made by two other models, which indicates a more accurate  
372 prediction of flood susceptibility in this area.

373

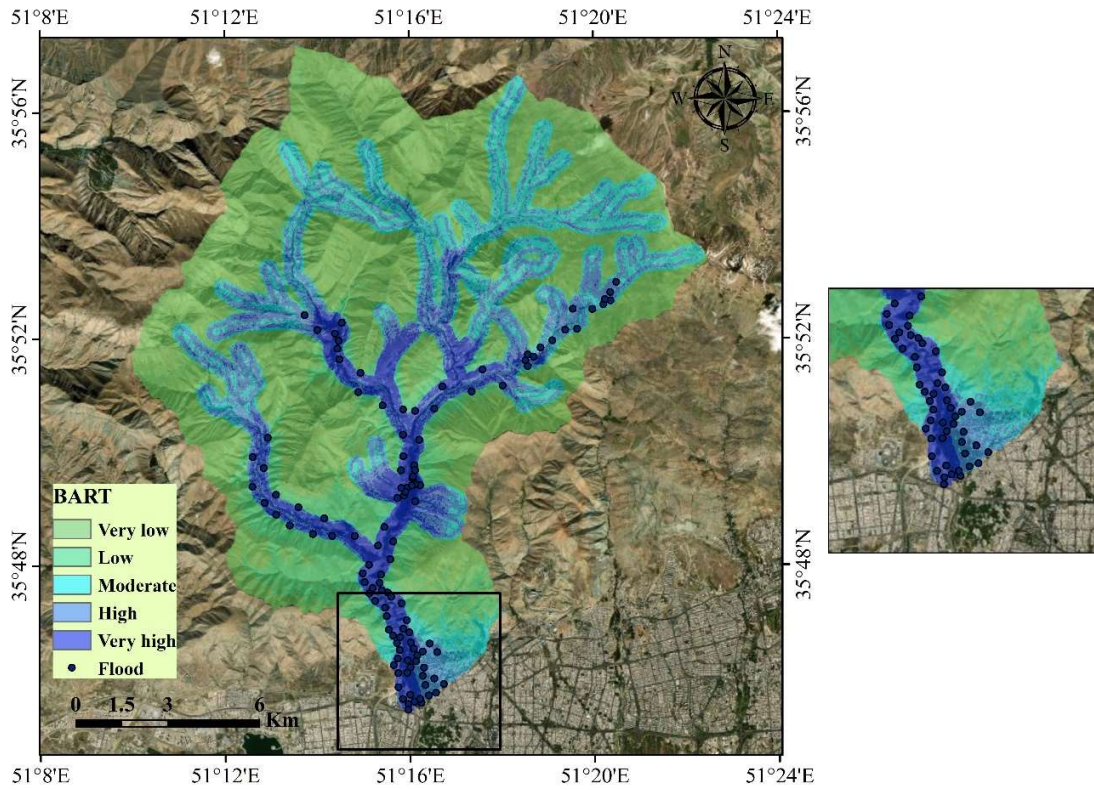


374



375

376



377

378

**Fig. 11. Flood susceptibility map using the Naïve Bayes, RF and BART models**

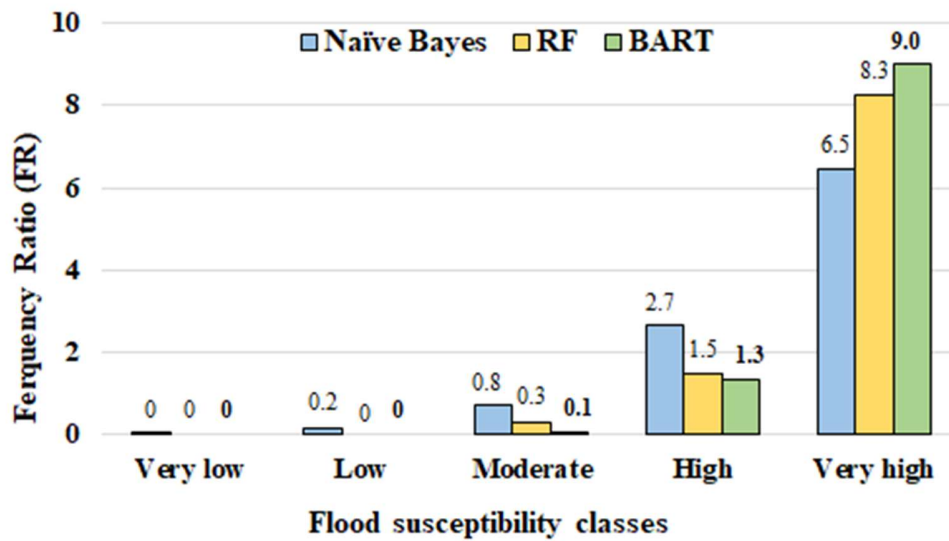
379

**Table 5. The watershed area (in km<sup>2</sup> and %) in each flood susceptibility class**

Susceptibility class	NB model		RF model		BART model	
	Area (km <sup>2</sup> )	Area (%)	Area (km <sup>2</sup> )	Area (%)	Area (km <sup>2</sup> )	Area (%)
Very low	121.85	56.52	112.32	52.10	106	49.17
Low	31.53	14.62	33.24	15.42	28.39	13.17
Moderate	21.67	10.05	31.04	14.40	30.65	14.22
High	18.44	8.55	17.77	8.24	31.08	14.42
Very High	22.11	10.26	21.23	9.85	19.48	9.04

380

381



382

383 Fig. 12. Analysis of the frequency of floods on the flood susceptibility maps predicted using the FR method

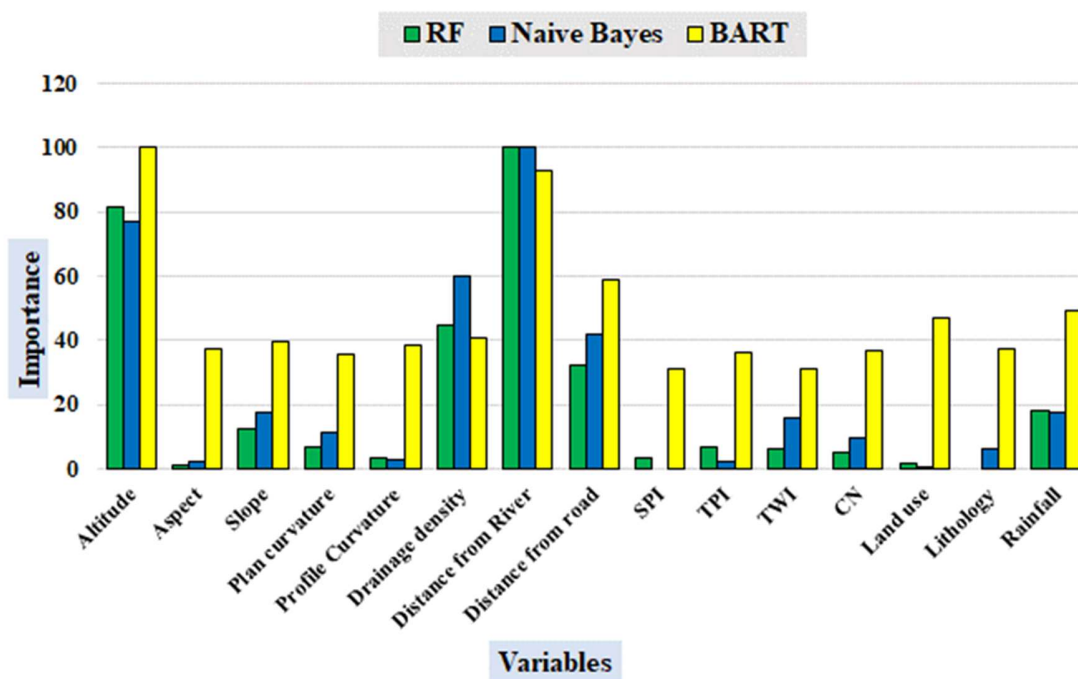
384 **3.5. Explanatory Variable Importance**

385 The results of the importance of the independent (i.e. input) variables used to model the flood  
 386 susceptibility using the three models are shown in Fig. 13. It is clear that in the three models used  
 387 different input variables have different effects on determining the flood susceptibility. It is also  
 388 clear that altitude and distance from the river are more important than other variables in all three  
 389 models.

390 Due to the importance of 4 variables (altitude, distance from the river, distance from the road and  
 391 rainfall) on flood susceptibility in the BART model, these 4 variables were further investigated  
 392 (Fig. 14). As it can be seen from Fig. 14, the flood susceptibility decreases with increasing altitude,  
 393 with highest sensitivity to floods being at an altitude of 1400 meters (which is close to the altitude  
 394 of the outlet of the watershed). This indicates the inverse relationship between the altitude and the  
 395 flooding susceptibility. Further, a study of the distance from the river shows that locations with  
 396 distances smaller than 500 meters have a high susceptibility to flooding whilst locations with

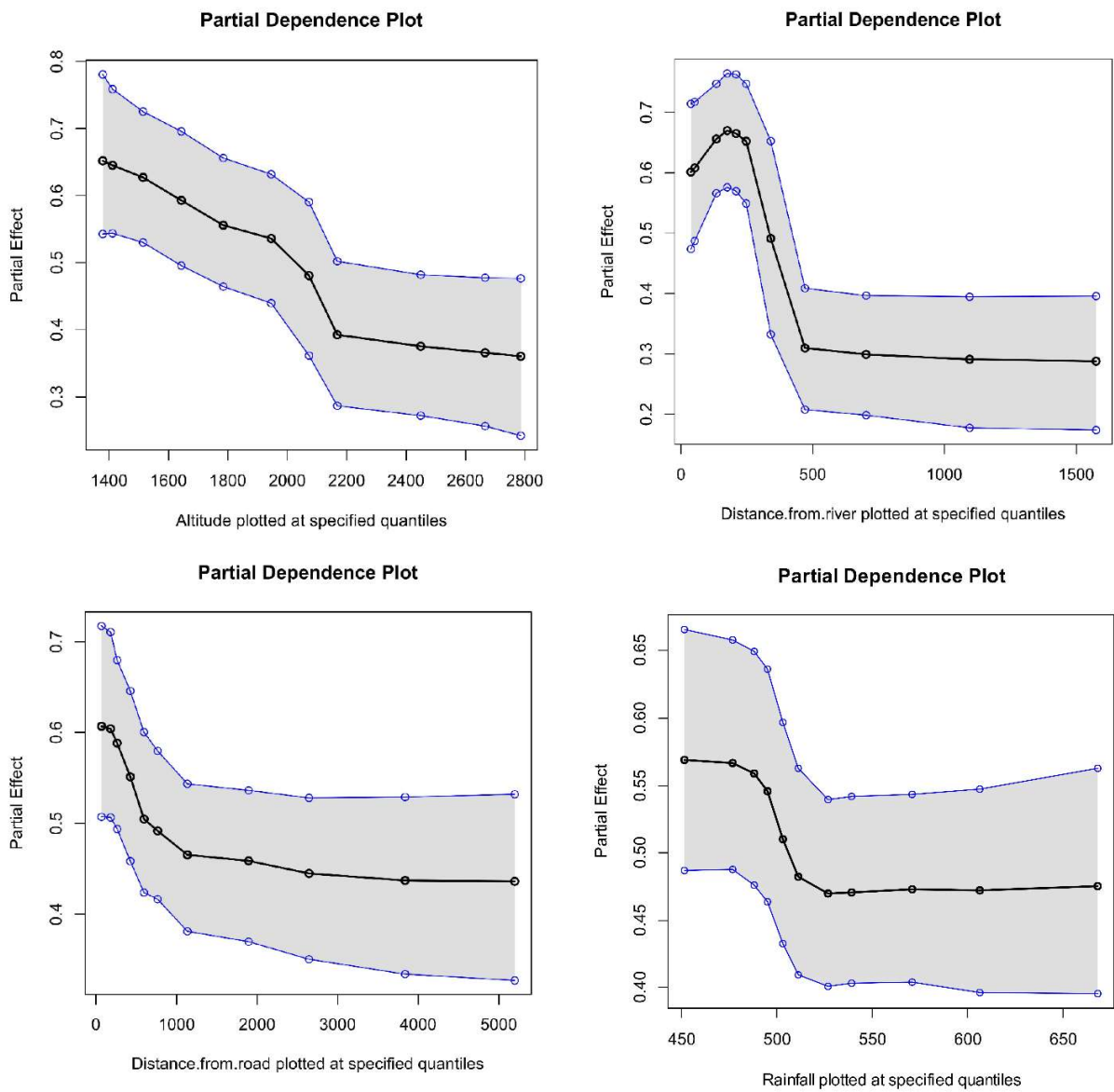
397 distances larger than 500 meters from the river have a decreasing flooding susceptibility which  
 398 stabilizes around a low value for the distances of 1000-1500 meters. Regarding the distance from  
 399 the road, it can be noted from Fig 14 that the flooding susceptibility decreases with the increasing  
 400 distance from the road with most sensitive areas being located less than 1000 meters from the road.  
 401 Finally, a study of the effect of rainfall on flooding susceptibility shows that areas with 450 to 500  
 402 mm of rainfall per year are more sensitive than the areas with higher rainfall (the susceptibility  
 403 decreases so that from rainfall 550 to 650 mm it is low and constant).

404



405

406 **Fig. 13. Results of relative importance of independent variables in flood sensitivity modeling in Naïve Bayes,**  
 407 **RF and BART models**



408

409 **Fig 14. Partial effect plot for four importance variable (altitude, distance from river, distance from road and**  
 410 **rainfall)**

411

412 **4. Discussion**

413 In the present study, we developed and presented a novel flood susceptibility BART model that is  
 414 based on machine learning and Bayesian approach. In addition, two existing models, NB and RF

415 were used for comparison. The results obtained showed that all three models have a high  
416 performance in predicting the flooding susceptibility in the Kan watershed in Iran but, based on  
417 the model performance criteria, the new BART model has outperformed the other two models. In  
418 terms of input variable importance, the results obtained show that the altitude and distance from  
419 the river are the most important variables for assessing flooding susceptibility in the study area.

420 One of the main objectives of this study was to apply the BART model and evaluate the efficiency  
421 of this model in flood modeling in the study area. Performance evaluation of NB, RF, and BART  
422 models shows that the BART model performed best in the validation stage in terms of predicting  
423 flood susceptibility. The use of the Bart model in Natural Hazard studies and especially flood  
424 sensitivity modeling has been reported rarely before. The efficiency of this model has been proven  
425 in other fields such as forest science. Ahmadi et al. (2021) used BART model to mapping forest  
426 stand characteristics and showed that this model has a high performance in comparison to other  
427 models.

428 The BART model is a non-parametric Bayesian regression approach that uses consistent basic  
429 random elements. Bayesian Additive Regression Trees (BART) provides a flexible way to fit a  
430 variety of regression models while avoiding strong parametric assumptions (Hill et al. 2020). The  
431 tree ensemble model is supported by an uncertainty framework in the Bayesian inferential  
432 framework and provides a principled approach to regulation through previous specifications  
433 (Pratola and Higdon 2016; Sparapani et al. 2016). This model uses a non-parametric tree  
434 aggregation model to allow flexibility of the average structure of a regression. But it also has the  
435 advantages of a Bayesian inferential framework given the amount of uncertainty and its regulation  
436 through calibrated data locations (Sparapani et al. 2016; Hill et al. 2020; Prado et al. 2021; Wu et  
437 al. 2021).



438 One of the main advantages of the BART model is the capacity to form inference on numerous  
439 features of the survival distribution directly from the posterior samples. As a Bayesian model,  
440 BART consists of a set of priors for the construction and the leaf parameters and a possibility for  
441 data in the terminal nodes (Pratola and Higdon 2016; Sparapani et al. 2016). The object of the  
442 priors is to afford regularization, limiting any single regression tree from dominating the total fit.  
443 Many Machine learning (ML) models suffer from missing data problems. BART model has a  
444 specialty that provides the user with the straight designation missing covariate data within the  
445 BART structure. This method combines missing data indicators into the training data set and  
446 supports for divisions on the missing indicators, guiding to raised efficiency under a pattern  
447 ensemble model structure (Hill et al. 2020; Prado et al. 2021; Sparapani et al. 2021).

448 Determining the importance of independent variables in flood susceptibility modeling in the Kan  
449 watershed showed that altitude, distance from river, distance from road and rainfall variables are  
450 important factors affecting flood susceptibility in this region. A study of altitude variable shows  
451 that low altitudes, which are often at the outlet of watersheds, are highly susceptible to flooding,  
452 which is consistent with the findings of Khosravi et al. (2019), Pham et al., (2020a).

453 Distance from river is another important factor in flood susceptibility in the Kan watershed, and  
454 the results indicate the sensitivity of areas close to the river. Ahmadlou et al., (2019) showed in  
455 their studies that areas 500-1000 meters from the river are highly sensitive to flooding. Given that  
456 the flood-prone areas are located near the river and the reason is due to rise of flow from the river  
457 channels (Choubin et al. 2019; Darabi et al. 2019; Panahi et al. 2021), in the Kan watershed, due  
458 to lack of observance of riverbed and river boundaries, several restaurants and villas have been  
459 built in the areas near the river, and due to the presence of more orchard in the river area, has led  
460 to the obstruction of flow in these areas and has increased the sudden release of flood current.

461 Invasion of the river boundaries and the create of orchard in it, in addition to causing financial  
462 damage to the residents of the area, also by blocking the flow in sections such as tunnels, will  
463 cause secondary floods and intensify the damage to the people and downstream areas.

464 Another factor affecting the flood susceptibility in the Kan watershed is the distance from road.  
465 Construction and crate of communication roads will increase the runoff and runoff speed because  
466 it will reduce the area of the existing surface to absorb rainfall and thus will increase the sensitivity  
467 to flooding in these areas (Tehrany et al. 2019b; Zhao et al. 2019).

468 The study of the rainfall indicates that areas with less rainfall are highly susceptible to flood, which  
469 are mainly areas close to the outlet of the Kan watershed. Due to the mountainous nature of the  
470 region, most of the precipitation in the upstream areas of the Kan watershed is snow, so in these  
471 areas the possibility of infiltration is higher. In addition, precipitation in the downstream areas is  
472 in the form of storms and these storms are usually more severe in the autumn and causes the river  
473 inundation and flooding.

474 In recent years, due to human interventions and the resulting climate and land-use changes, the  
475 rate of flooding and the corresponding damages have increased significantly. Studies such as this  
476 one allow managers to reduce flood risks through planning and flood susceptibility analysis.  
477 Therefore, we are always looking for more accurate modeling approaches to reduce the bias in the  
478 prediction of flood susceptibility. In the present study, we showed that BART model is an accurate  
479 model that can be used for effective flood susceptibility modeling. This model can be applied in  
480 the future along with other modes that have shown high ability in flood modeling studies.

481

## 482 **5. Conclusion**

483 Floods are one of the most frequent and destructive natural disasters that can cause a lot of damage.  
484 In order to investigate and analyze the susceptibility of some are to flooding, different methods  
485 have been developed by the researchers.

486 In this study, the Bayesian based model (Naïve Bayes), regression tree type model (Random  
487 Forest) and ensemble type model (Bayesian Additive Regression Tree - BART) were developed  
488 to predict flood susceptibility in the Kan watershed. A total of 15 explanatory (i.e. model input)  
489 variables were used after multi-collinearity analyses as independent variables and 118 flood  
490 locations and 115 non-flood locations after field surveys and the use of available information as a  
491 dependent variable for flood modeling.

492 The validation results obtained for flood susceptibility modeling showed that the Naïve Bayes, RF  
493 and BART models all have a good predictive performance. However, the new BART model has  
494 the higher prediction accuracy than the Naïve Bayes and RF models. This is due to the fact that it  
495 uses features of both methods in the ensemble setting.

496 The analysis of the importance of explanatory variables showed that the effect of independent  
497 variables is different in each model. However, the altitude and distance from the river were more  
498 important than other variables in all three models meaning that low-height areas and areas close to  
499 the river are more susceptible to flooding.

500 The Kan watershed is close to the city of Tehran and the pleasant climate of this tourist area has  
501 caused that its riverbanks are occupied with many constructions that have been carried out. These  
502 areas receive a large number of tourists in spring and summer and hence are strongly affected by  
503 the floods. It is therefore necessary to provide flood hazard maps for the region. The results of this

504 research can be used as a baseline map in development projects to determine areas susceptible to  
505 flooding hence prevent the construction in these high-risk areas.

506 **Author Contributions:** Saeid Janizadeh acquired the data; Saeid Janizadeh and Mehdi Vafakhah  
507 conceptualized and performed the analysis; Saeid Janizadeh wrote the manuscript and discussion,  
508 and analyzed the data; Mehdi Vafakhah, Zoran Kapelan and Naghmeh Mobarghaee Dinan  
509 provided technical sights, as well as edited, restructured, and professionally optimized the  
510 manuscript. All authors discussed the results and edited the manuscript. All authors have read and  
511 agreed to the published version of the manuscript.

512 **Ethical Approval:** We confirm that this manuscript has not been published elsewhere and is not  
513 under consideration by another journal.

514 **Consent to Participate:** All authors have participated the manuscript and agree with submission  
515 to Water Resources Management.

516 **Consent to Publish:** All authors have approved the publication of this manuscript in the Water  
517 Resources Management Journal.

518 **Availability of data and materials:** We have no permission to release data and codes.

519

520 **Funding:** The authors received no specific funding for this work.

521 **Acknowledgments:** We acknowledge Tarbiat Modares University's support for this work.

522 **Conflicts of Interest:** The authors declare no conflict of interest.

## 523 **References**

524 Ahmadlou M, Karimi M, Alizadeh S, et al (2019) Flood susceptibility assessment using integration of  
525 adaptive network-based fuzzy inference system (ANFIS) and biogeography-based optimization

526 (BBO) and BAT algorithms (BA). *Geocarto Int* 34:1252–1272

527 Al-Abadi AM (2018) Mapping flood susceptibility in an arid region of southern Iraq using ensemble  
528 machine learning classifiers: a comparative study. *Arab J Geosci* 11:218

529 Al-Juaidi AEM, Nassar AM, Al-Juaidi OEM (2018) Evaluation of flood susceptibility mapping using  
530 logistic regression and GIS conditioning factors. *Arab J Geosci* 11:765

531 Arabameri A, Saha S, Chen W, et al (2020) Flash flood susceptibility modelling using functional tree and  
532 hybrid ensemble techniques. *J Hydrol* 125007

533 Bui DT, Panahi M, Shahabi H, et al (2018) Novel hybrid evolutionary algorithms for spatial prediction of  
534 floods. *Sci Rep* 8:15364

535 Chapi K, Singh VP, Shirzadi A, et al (2017) A novel hybrid artificial intelligence approach for flood  
536 susceptibility assessment. *Environ Model Softw* 95:229–245

537 Chen W, Li Y, Xue W, et al (2020) Modeling flood susceptibility using data-driven approaches of  
538 naive bayes tree, alternating decision tree, and random forest methods. *Sci Total Environ*  
539 701:134979

540 Choubin B, Moradi E, Golshan M, et al (2019) An ensemble prediction of flood susceptibility using  
541 multivariate discriminant analysis, classification and regression trees, and support vector machines.  
542 *Sci Total Environ* 651:2087–2096

543 Chowdhuri I, Pal SC, Arabameri A, et al (2020) Implementation of artificial intelligence based ensemble  
544 models for gully erosion susceptibility assessment. *Remote Sens* 12:3620

545 Cook A, Merwade V (2009) Effect of topographic data, geometric configuration and modeling approach  
546 on flood inundation mapping. *J Hydrol* 377:131–142

547 Costache R (2019) Flash-flood Potential Index mapping using weights of evidence, decision Trees  
548 models and their novel hybrid integration. *Stoch Environ Res Risk Assess* 33:1375–1402

549 Costache R, Arabameri A, Blaschke T, et al (2021) Flash-Flood Potential Mapping Using Deep Learning,  
550 Alternating Decision Trees and Data Provided by Remote Sensing Sensors. *Sensors* 21:280.  
551 <https://doi.org/10.3390/s21010280>

552 Costache R, Bui DT (2020) Identification of areas prone to flash-flood phenomena using multiple-criteria  
553 decision-making, bivariate statistics, machine learning and their ensembles. *Sci Total Environ*  
554 712:136492

555 Darabi H, Choubin B, Rahmati O, et al (2019) Urban flood risk mapping using the GARP and QUEST  
556 models: A comparative study of machine learning techniques. *J Hydrol* 569:142–154

557 Delkash M, Al-Faraj FAM, Scholz M (2014) Comparing the export coefficient approach with the soil and  
558 water assessment tool to predict phosphorous pollution: the Kan watershed case study. *Water, Air,  
559 Soil Pollut* 225:2122

560 El-Magd SAA, Pradhan B, Alamri A (2021) Machine learning algorithm for flash flood prediction  
561 mapping in Wadi El-Laqeita and surroundings, Central Eastern Desert, Egypt. *Arab J Geosci* 14:1–  
562 14

563 Frattini P, Crosta G, Carrara A (2010) Techniques for evaluating the performance of landslide  
564 susceptibility models. *Eng Geol* 111:62–72

565 Heidari A (2014) Flood vulnerability of the K arun R iver S ystem and short-term mitigation measures. *J*  
566 *flood risk Manag* 7:65–80

567 Hill J, Linero A, Murray J (2020) Bayesian additive regression trees: A review and look forward. *Annu*  
568 *Rev Stat Its Appl* 7:251–278

569 Hong H, Panahi M, Shirzadi A, et al (2018) Flood susceptibility assessment in Hengfeng area coupling  
570 adaptive neuro-fuzzy inference system with genetic algorithm and differential evolution. *Sci Total*  
571 *Environ* 621:1124–1141

572 Hooshyaripor F, Faraji-Ashkavar S, Koohyian F, et al (2020) Annual flood damage influenced by El Niño  
573 in the Kan River basin, Iran. *Nat Hazards Earth Syst Sci* 20:2739–2751

574 Hosseini FS, Choubin B, Mosavi A, et al (2020) Flash-flood hazard assessment using ensembles and  
575 Bayesian-based machine learning models: application of the simulated annealing feature selection  
576 method. *Sci Total Environ* 711:135161

577 Islam ARMT, Talukdar S, Mahato S, et al (2021) Flood susceptibility modelling using advanced

578 ensemble machine learning models. *Geosci Front* 12:101075

579 Janizadeh S, Avand M, Jaafari A, et al (2019) Prediction Success of Machine Learning Methods for Flash  
580 Flood Susceptibility Mapping in the Tafresh Watershed, Iran. *Sustainability* 11:5426

581 Kalantar B, Ueda N, Saeidi V, et al (2021) Deep Neural Network Utilizing Remote Sensing Datasets for  
582 Flood Hazard Susceptibility Mapping in Brisbane, Australia. *Remote Sens* 13:2638

583 Kapelner A, Bleich J (2013) bartMachine: Machine learning with Bayesian additive regression trees.  
584 arXiv Prepr arXiv13122171

585 Khosravi K, Pham BT, Chapi K, et al (2018) A comparative assessment of decision trees algorithms for  
586 flash flood susceptibility modeling at Haraz watershed, northern Iran. *Sci Total Environ* 627:744–  
587 755

588 Khosravi K, Pourghasemi HR, Chapi K, Bahri M (2016) Flash flood susceptibility analysis and its  
589 mapping using different bivariate models in Iran: a comparison between Shannon’s entropy,  
590 statistical index, and weighting factor models. *Environ Monit Assess* 188:656

591 Khosravi K, Shahabi H, Pham BT, et al (2019) A comparative assessment of flood susceptibility  
592 modeling using Multi-Criteria Decision-Making Analysis and Machine Learning Methods. *J Hydrol*  
593 573:311–323

594 Liaw A, Wiener M, others (2002) Classification and regression by randomForest. *R news* 2:18–22

595 Liu R, Chen Y, Wu J, et al (2016) Assessing spatial likelihood of flooding hazard using naïve Bayes  
596 and GIS: a case study in Bowen Basin, Australia. *Stoch Environ Res risk Assess* 30:1575–1590

597 Mahmoud SH, Gan TY (2018) Multi-criteria approach to develop flood susceptibility maps in arid  
598 regions of Middle East. *J Clean Prod* 196:216–229

599 Miles J (2014) Tolerance and variance inflation factor. *Wiley StatsRef Stat Ref Online*

600 Molinos-Senante M, Hernández-Sancho F, Sala-Garrido R (2011) Cost-benefit analysis of water-reuse  
601 projects for environmental purposes: A case study for Spanish wastewater treatment plants. *J*  
602 *Environ Manage* 92:3091–3097

603 Ngo P-T, Hoang N-D, Pradhan B, et al (2018) A Novel Hybrid Swarm Optimized Multilayer Neural

604 Network for Spatial Prediction of Flash Floods in Tropical Areas Using Sentinel-1 SAR Imagery  
605 and Geospatial Data. *Sensors* 18:3704. <https://doi.org/10.3390/s18113704>

606 Panahi M, Dodangeh E, Rezaie F, et al (2021) Flood spatial prediction modeling using a hybrid of meta-  
607 optimization and support vector regression modeling. *Catena* 199:105114

608 Papaioannou G, Vasiliades L, Loukas A (2015) Multi-criteria analysis framework for potential flood  
609 prone areas mapping. *Water Resour Manag* 29:399–418

610 Pham BT, Avand M, Janizadeh S, et al (2020a) GIS Based Hybrid Computational Approaches for Flash  
611 Flood Susceptibility Assessment. *Water* 12:683

612 Pham BT, Phong T Van, Nguyen HD, et al (2020b) A Comparative Study of Kernel Logistic Regression,  
613 Radial Basis Function Classifier, Multinomial Naïve Bayes, and Logistic Model Tree for Flash  
614 Flood Susceptibility Mapping. *Water* 12:239

615 Plant E, King R, Kath J (2021) Statistical comparison of additive regression tree methods on ecological  
616 grassland data. *Ecol Inform* 61:101198

617 Prado EB, Moral RA, Parnell AC (2021) Bayesian additive regression trees with model trees. *Stat*  
618 *Comput* 31:1–13

619 Prasad P, Loveson VJ, Das B, Kotha M (2021) Novel Ensemble Machine Learning Models in Flood  
620 Susceptibility Mapping. *Geocarto Int* 1–22. <https://doi.org/10.1080/10106049.2021.1892209>

621 Pratola MT, Higdon DM (2016) Bayesian additive regression tree calibration of complex high-  
622 dimensional computer models. *Technometrics* 58:166–179

623 Rahmati O, Pourghasemi HR, Zeinivand H (2016) Flood susceptibility mapping using frequency ratio and  
624 weights-of-evidence models in the Golastan Province, Iran. *Geocarto Int* 31:42–70

625 Rish I, others (2001) An empirical study of the naive Bayes classifier. In: *IJCAI 2001 workshop on*  
626 *empirical methods in artificial intelligence*. pp 41–46

627 Shafapour Tehrany M, Shabani F, Neamah Jebur M, et al (2017) GIS-based spatial prediction of flood  
628 prone areas using standalone frequency ratio, logistic regression, weight of evidence and their  
629 ensemble techniques. *Geomatics, Nat Hazards Risk* 8:1538–1561



630 Shafizadeh-Moghadam H, Valavi R, Shahabi H, et al (2018) Novel forecasting approaches using  
631 combination of machine learning and statistical models for flood susceptibility mapping. *J Environ*  
632 *Manage* 217:1–11

633 Shahabi H, Shirzadi A, Ghaderi K, et al (2020) Flood detection and susceptibility mapping using sentinel-  
634 1 remote sensing data and a machine learning approach: Hybrid intelligence of bagging ensemble  
635 based on k-nearest neighbor classifier. *Remote Sens* 12:266

636 Sparapani R, Spanbauer C, McCulloch R (2021) Nonparametric machine learning and efficient  
637 computation with bayesian additive regression trees: the BART R package. *J Stat Softw* 97:1–66

638 Sparapani RA, Logan BR, McCulloch RE, Laud PW (2016) Nonparametric survival analysis using  
639 Bayesian additive regression trees (BART). *Stat Med* 35:2741–2753

640 Talukdar S, Ghose B, Salam R, et al (2020) Flood susceptibility modeling in Teesta River basin,  
641 Bangladesh using novel ensembles of bagging algorithms. *Stoch Environ Res Risk Assess* 34:2277–  
642 2300

643 Tang X, Li J, Liu M, et al (2020) Flood susceptibility assessment based on a novel random Na<sup>i</sup>ve  
644 Bayes method: A comparison between different factor discretization methods. *Catena* 190:104536

645 Tang Z, Yi S, Wang C, Xiao Y (2018) Incorporating probabilistic approach into local multi-criteria  
646 decision analysis for flood susceptibility assessment. *Stoch Environ Res risk Assess* 32:701–714

647 Tehrany MS, Jones S, Shabani F (2019a) Identifying the essential flood conditioning factors for flood  
648 prone area mapping using machine learning techniques. *Catena* 175:174–192

649 Tehrany MS, Kumar L (2018) The application of a Dempster--Shafer-based evidential belief function in  
650 flood susceptibility mapping and comparison with frequency ratio and logistic regression methods.  
651 *Environ Earth Sci* 77:490

652 Tehrany MS, Kumar L, Shabani F (2019b) A novel GIS-based ensemble technique for flood  
653 susceptibility mapping using evidential belief function and support vector machine: Brisbane,  
654 Australia. *PeerJ* 7:e7653

655 Tehrany MS, Pradhan B, Jebur MN (2014) Flood susceptibility mapping using a novel ensemble weights-

656 of-evidence and support vector machine models in GIS. *J Hydrol* 512:332–343

657 Tehrany MS, Pradhan B, Mansor S, Ahmad N (2015) Flood susceptibility assessment using GIS-based  
658 support vector machine model with different kernel types. *Catena* 125:91–101

659 Vafakhah M, Loor SMH, Pourghasemi H, Katebikord A (2020) Comparing performance of random forest  
660 and adaptive neuro-fuzzy inference system data mining models for flood susceptibility mapping.  
661 *Arab J Geosci* 13:417

662 Vetrivel A, Gerke M, Kerle N, et al (2018) Disaster damage detection through synergistic use of deep  
663 learning and 3D point cloud features derived from very high resolution oblique aerial images, and  
664 multiple-kernel-learning. *ISPRS J Photogramm Remote Sens* 140:45–59

665 Woodward M, Kapelan Z, Gouldby B (2014) Adaptive flood risk management under climate change  
666 uncertainty using real options and optimization. *Risk Anal* 34:75–92

667 Wu W, Tang X, Lv J, et al (2021) Potential of Bayesian additive regression trees for predicting daily  
668 global and diffuse solar radiation in arid and humid areas. *Renew Energy*

669 Yariyan P, Janizadeh S, Van Phong T, et al (2020) Improvement of Best First Decision Trees Using  
670 Bagging and Dagging Ensembles for Flood Probability Mapping. *Water Resour Manag* 1–17

671 Yesilnacar E, Topal T (2005) Landslide susceptibility mapping: a comparison of logistic regression and  
672 neural networks methods in a medium scale study, Hendek region (Turkey). *Eng Geol* 79:251–266

673 Zhang H (2004) The Optimality of Naive Bayes, 2004. *Am Assoc Artif Intell* ([www.aaai.org](http://www.aaai.org))

674 Zhao G, Pang B, Xu Z, et al (2019) Assessment of urban flood susceptibility using semi-supervised  
675 machine learning model. *Sci Total Environ* 659:940–949

676